Available online at www.sciencedirect.com
SCIENCE DIRECT®
Journal of the European Ceramic Society 25 (2005) 3523–3531
www.elsevier.com/locate/jeurceramsoc

Analysis of acoustic emission signature during aluminous cement setting to characterise the mechanical behaviour of the hard material

T. Chotard[a,b,*], D. Rotureau[a], A. Smith[a,**]

[a] *Groupe d'Etude des Matériaux Hétérogènes (GEMH, EA 3178), Ecole Nationale Supérieure de Céramique Industrielle, 47 à 73 Avenue Albert Thomas, 87065 Limoges Cedex, France*
[b] *Département Génie Mécanique et Productique, Institut Universitaire de Technologie, 2 allée André Maurois, 87065 Limoges Cedex, France*

Received 28 May 2004; received in revised form 22 September 2004; accepted 24 September 2004
Available online 15 December 2004

Abstract

In this paper, the application of acoustic emission (AE) technique during cement hydration is used to predict the mechanical behaviour of the set material. This non-destructive and in situ method widely used in damage characterisation and more recently, in material process monitoring. It permits the cement hydration to be followed at early age from a few minutes to a few hours after mixing. The AE signals concerning two lots of aluminous cement paste (water to cement weight ratio: 0.4; temperature of measurement: 20 °C) with different ageing conditions were recorded and analysed. Mechanical testing was also conducted on set samples. Based on the experiments, the relationship between the AE features recorded during setting and the mechanical properties of the hard material was emphasised. The results showed that AE technique is a valuable tool to characterise and predict with a quite good reliability the mechanical performance of a set cement from its young age behaviour.

Keywords: Ageing; Calcium aluminate cement; Acoustic emission; Mechanical properties; Cements

1. Introduction

Calcium aluminate cements (CACs) are the basis of high performance materials and have found recent applications in sewage networks, hydraulic dams, refractories, low-cement castables or in building components (tile cements and self-levelling screeds).[1–3] These cements contain CaO and Al_2O_3 as the main oxides combined to give monocalcium aluminates (CA) as the major active phase in the anhydrous powder. This phase reacts with water to give calcium aluminate hydrates (CAH_{10}, C_2AH_8 and C_3AH_6) and also alumina hydrates (AH_3). One of the key issue with such materials is to be able to predict their mechanical behaviour and performances in service. The long-term behaviour of a cement paste is closely related to its state at the early age and in particular its hydration process. Since this period is essential, it has been very well studied over the past 10 years.[4,5] Most of characterisation techniques involved in these studies were ex situ (X-ray diffraction, differential thermal analysis, thermogravimetric measurements). However, in situ methods such as proton and aluminium nuclear magnetic resonance,[6] neutron diffraction[7–9] or ultrasonic measurements[10–12] can also give good results concerning this period. Recently,[13] acoustic emission (AE) technique has proved its ability, after performing both statistical and chronological AE data analysis, to characterise physical phenomena and chemical reactions taking place during the hydration process and that. One challenge with cement-based materials is to be able to predict from the early age behaviour its final performance. In this paper, we describe how AE can provide useful information about cement hydration and how this information can be cor-

* Corresponding author.
** Co-corresponding author.
E-mail addresses: t_chotard@ensci.fr (T. Chotard), a_smith@ensci.fr (A. Smith).

0955-2219/$ – see front matter © 2004 Elsevier Ltd. All rights reserved.
doi:10.1016/j.jeurceramsoc.2004.09.019

related with the mechanical properties of the material in its hardened state. The AE technique, as used in this work, is a "passive technique" which utilises the AE signals generated by the physical and chemical changes occuring in the cement paste during the first 24 h.

2. Material and methods

2.1. Preparation of the cement paste

The cement is a commercial aluminous material whose composition and physical characteristics are given in Table 1.

The particle size distribution ranges between 0.3 and 100 μm with an average size around 10 μm. The results presented in this paper refer to cement manufactured at a given date but stored for different periods. After reception, cement A was stored at 20 °C and 40% relative humidity (RH) for two days and before testing. Cement B is a part of the same cement but stored in the same conditions for 55 days. Prior to mixing, a thermogravimetric analysis was performed on each lot of the anhydrous cement powder (A and B) in order to determine their weight losses between 20 and 1200 °C. Cement pastes were prepared to the same water-to-cement weight ratio (W/C), 0.4. The pastes were mixed according to the normalised procedure no. CEN 196-3. After mixing, the same quantities of paste for both cement A and cement B were poured in silicone foam moulds (100 mm × 100 mm × 30 mm) prior to AE measurements. Silicone foam has been selected since it can follow the shrinkage of the cement paste during setting. A possible separation between the mould and the tested material is reduced and the related parasitic noise in the AE signal is avoided. The AE characterisations have been carried out at 20 °C and 95% relative humidity. After AE measurements, the samples were re-stored under the same climatic conditions and during the same time (12 h at 20 °C and 40% RH). Then, cylinders were machined from the main samples and tested under indirect tensile loading. The reproducibility of data has been checked using several pastes made from the same cements.

2.2. Characterisation techniques

2.2.1. Acoustic emission

2.2.1.1. Background. Ultrasonic methods are widely used to perform in situ material characterisations.[14–16] AE technique has been developed over the last two decades as a non-destructive evaluation technique for material research.[17,18] AE is an efficient method to monitor, in real time, damage growth in both structural components and laboratory specimens. In loaded materials, the strain-energy release due to microstructural changes results in stress-wave propagation. AE is defined as "the class of phenomena whereby transient elastic waves are generated by the rapid release of energy from localised sources within a material (or structure) or the transient waves so generated". When a material is submitted to stresses (such as mechanical stresses, electric transients, etc.), acoustic emission can be generated by a variety of sources, including crack nucleation and propagation, multiple dislocation slip, twinning, grain boundary sliding, Barkhausen effect (realignment or growth of magnetic domains), phase transformations in alloys, debonding of fibres in composite materials or fracture of inclusions in alloys.[19–25] In the case of composite materials, many mechanisms have been confirmed as AE sources including matrix cracking, fibre–matrix interface debonding, fibre fracture and delamination.[26] AE deals with the detection of such waves at the materials surface. Therefore, this technique potentially allows not only the location of the source of the emission, but also the determination of its nature.

The stress waves resulting from microstructural changes depend on the propagation conditions including attenuation, damping and boundary surface interactions in a heterogeneous medium. The signal delivered by the sensor is not an exact representation of the original source. Nevertheless, it is realistic to consider that this signal contains some features representative of the source in such a manner that direct correlations exist between the internal mechanisms and the magnitude of the various AE parameters. Consequently, each signal can be considered as the acoustic signature of different phenomena. In the case of concrete structures submitted to mechanical loading, AE events occur when cracks

Table 1
Chemical composition, either in nature of cementitous phase or in oxide, for the cement

Chemical composition		Percentage (wt. %)
Cementitous phase	$CaAl_2O_4$ (or CA)	56
	$CaAl_4O_7$ (or CA_2)	38
	Al_2O_3	< 6
	$Ca_{12}Al_{14}O_{33}$ (or $C_{12}A_7$)	< 1
Oxide	CaO	26.6 – 29.2
	Al_2O_3	69.8 – 72.2

develop in the concrete and stress waves are emitted.[27,28] Research activities about AE has been applied to concrete either to characterise crack development or to monitor plain structure. Concerning the first aspect, i.e. crack development, AE has been used to observe the fracture process zone (FPZ) that develops ahead of the crack tip,[29] to describe the fracture mechanisms or to locate the cracks and their type of propagation.[30] Conventional AE source location methods are typically used to spatially locate crack development,[31] whereas moment tensor analysis has been applied to identify the location of the source and orientation of the damage.[32] When coupled with normalised mechanical testing of materials, AE enables the determination not only of the existence of damage, but also of the type and extent of damage. From this information, attempts have been made to infer the location of specimen failure and the probable mechanisms of failure. With respect to the second aspect, i.e. monitoring of structures, several researchers have suggested the use of AE either to assess the degree of damage or as a method to monitor structural integrity.[33] In the present work, the use of AE technique will be devoted to record the elastic waves emitted during the physical and chemical changes that occur throughout the hydration of the cement paste. The specificity here is two-fold:

(1) Characterisation is done on a paste that transforms into a solid,
(2) No external load is applied on the system under study.

The potential of acoustic emission for providing reliable information and the ease with which it is applied for in situ testing depend largely on the available AE instrumentation. Significant improvements and modifications have been made on acoustic emission systems including features for numerical acquisition and analyses. From the emitted signals, different data can be extracted, such as number of hits (i.e. the recorded signal), number of counts (i.e. the number of alternation in a single hit), rise time or peak amplitude. Fig. 1 presents the typical AE features extracted from the signal waveform. Different types of analysis can also be done concerned with amplitude, duration, energy and frequency.

2.2.1.2. Experimental set-up. Acoustic emission was continuously monitored during cement early age (from 0 to 24 h) by using a Mistras 2001 data acquisition system of Physical Acoustics Corporation (PAC), with a sampling rate of 8 MHz and a 40 dB pre-amplification. The total amplification of the recording system was 80 dB. Ambient noise was filtered using a threshold of 35 dB. AE measurements were achieved by using two resonant R15 PAC sensors, one as test sensor and one as reference sensor. The reference sensor is used in order to record noise arising from the electromagnetic environment and to eventually subtract these parasitic signals from that recorded on the test sensor. A coupling fluid (Dough 428 Rhodorsil Silicone) is used to have an airless and flawless contact between the transducer and the specimen; Fig. 2 shows the experimental set up.

2.2.2. Indirect tensile test

Since some difficulties are encountered in testing brittle materials in direct tension, indirect methods become attractive. Indirect tensile test was here performed in order to determine the tensile strength of the set cements. In his review, Darwell[34] described a cylinder split routine testing for the tensile strength of concrete. Fig. 3 shows the experimental configuration of this kind of test. The sample is a cylinder that has a length over diameter ratio (L/D) ranging between 1 and 5. This condition must be respected in order to avoid buckling or unexpected shear stress distribution. In our case, and considering the thickness of the set cement samples, cylinders of 30 mm length with a diameter of 20 mm were machined with a core sampler as presented in Fig. 4.

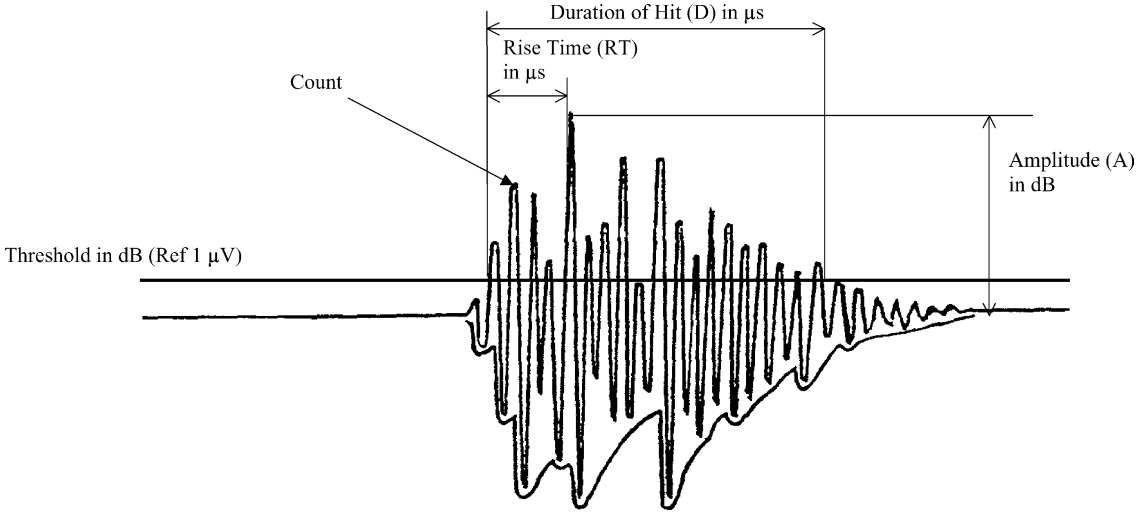

Fig. 1. Typical AE signal recorded with its associated characteristics.

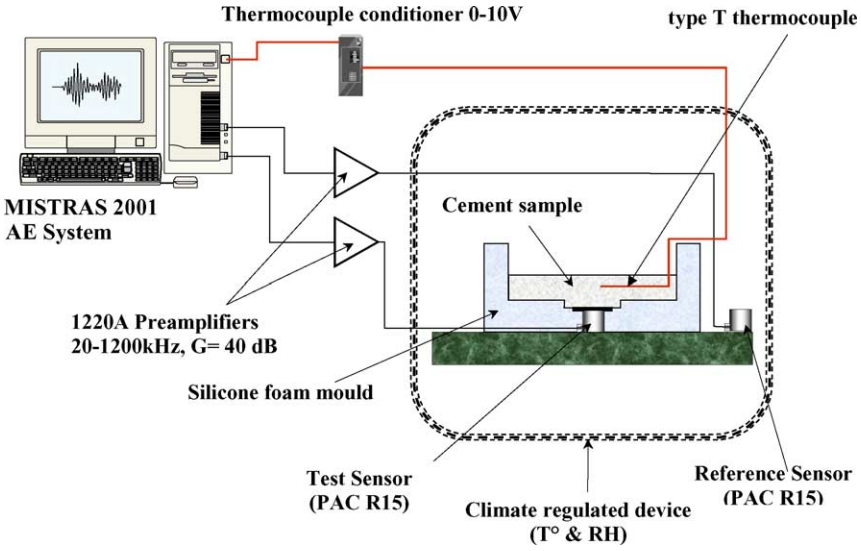

Fig. 2. Experimental set-up for AE testing.

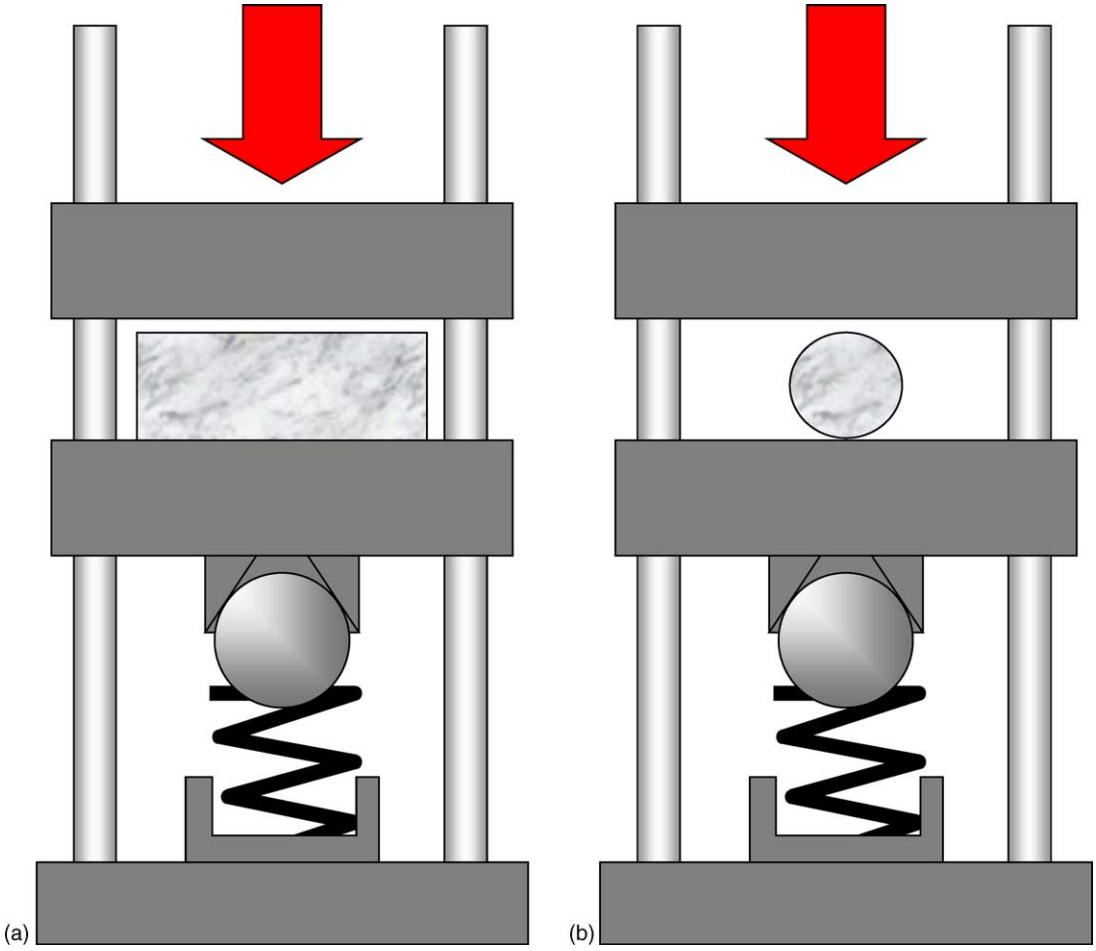

Fig. 3. Experimental set-up for indirect tensile test: (a) front view and (b) side view.

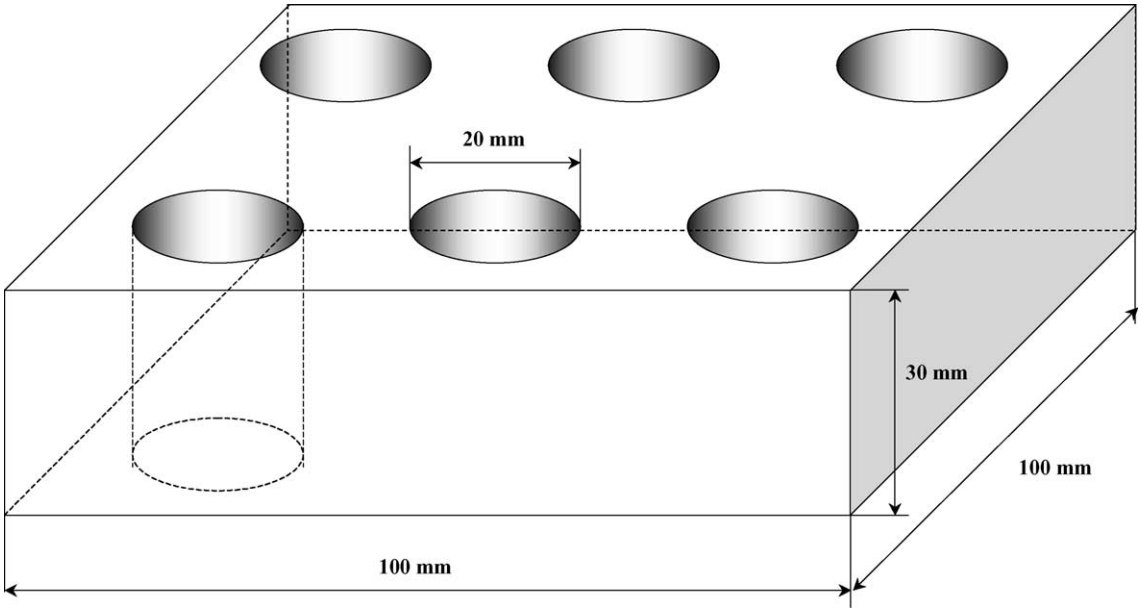

Fig. 4. Scheme of core sampling in set cement samples.

Once the tests performed, the tensile strength is calculated using the basic equation which derives from Hertzian theory:

$$\sigma_t = \frac{2P}{\pi DL} \quad (1)$$

where P is the load at failure, D the diameter of the cylinder and L its length.

3. Results and discussion

3.1. AE testing

Fig. 5 presents typical curves reporting the variations of the AE cumulative hit as a function of time after mixing cement A and cement B. The first observation is relative to the cumulative number of hits which is more important for cement A than for cement B (nearly twice more). This is characteristic of a high acoustic activity taking place in the sample probably related to the number of physical events and chemical reactions occurring during hydration. A second observation concerns the rate of variation that is greater in the case of cement A than cement B. We will discuss about the interpretation of this later. A more precise analysis was performed on both AE data and internal temperature data measured in cement in order to characterise the differences in AE activity occurring during the setting period. Several parameters were either determined from the curves or calculated as shown on Fig. 6. t_T^{Start} and t_{AE}^{Start} refer to the times when there is a significant modification of slope for T and the number of cumulative hits, respectively. t_T^{Max} corresponds to the time when the internal temperature reaches its maximum value (T^{max}), $\partial T/\partial t$ is the internal temperature rate during the increase of temperature and $\partial H/\partial t$ is the AE hit rate. We deliberately do not discuss the decreasing of the internal temperature curve due to the influence of the specific thermal coefficient (diffusion) of the silicon foam mould, on the values obtained. Fig. 7a and b show the variations of the number of AE cumulative hits and the temperature as a function of time after mixing for the cement A and cement B, respectively. Table 2 reports the different values deduced from AE and temperature curves.

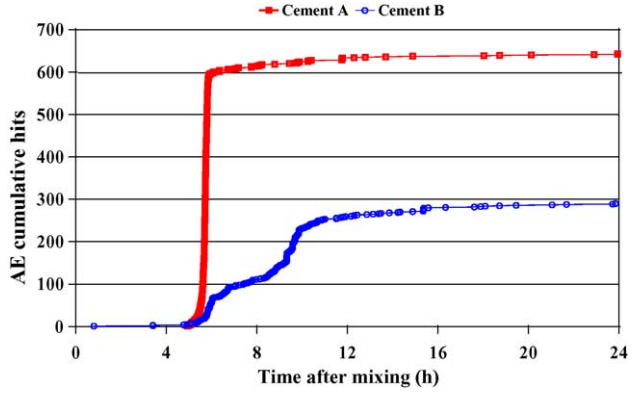

Fig. 5. AE cumulative hits as a function of time after mixing (cement A and cement B).

The AE feature variation for cement A (Fig. 7a) can be divided into three distinct periods. During the first one, from 0 to 4.92 h (t_{AE}^{Start}), no acoustic emission activity is recorded. If we look at the temperature variations in the same interval, we notice that the temperature starts increasing earlier ($t_T^{Start} = 2.70$ h) than AE rise ($t_T^{Start} < t_{AE}^{Start}$). Before t_T^{Start}, it has been founded that the cement is in its dormant period where the anhydrous phase dissolves and a small amount of hydrates starts to nucleate.[13] Another point concerning the variation of temperature must be underlined. A significant change in the temperature rate occurs at $t = 4.91$ h which is extremely

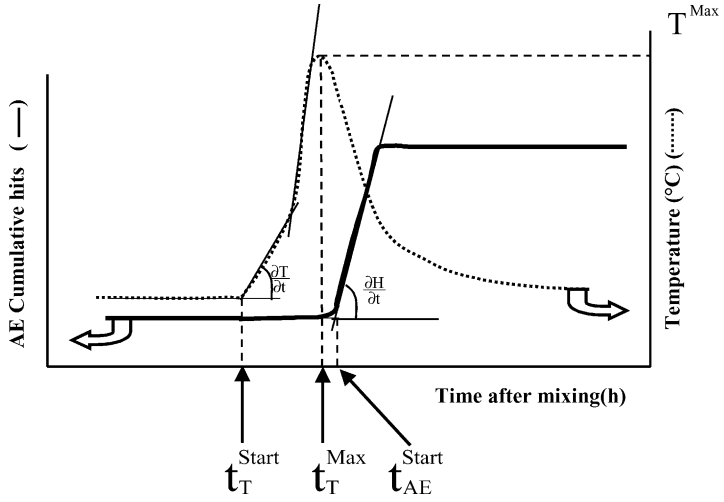

Fig. 6. Schematic representation of AE cumulative number of hits and internal temperature variations as a function of time after mixing. Description of the graphical determination of t_T^{Start}, t_T^{Max}, t_{AE}^{Start}, T^{max}, $\partial T/\partial t$ and $\partial H/\partial t$.

close to the value of t_{AE}^{Start} (4.92 h). As the internal temperature measured in a cement specimen is a marker of hydration reaction, we can assume that the exothermic phenomenon characterised by a notable rise of the internal temperature is closely related to the beginning of the precipitation of hydrates ($\partial T/\partial t = 5.3\,^{\circ}C/h$).

The second stage begins from 4.92 h to finish approximately at 6 h. During this period, and as the reaction pursues, a massive precipitation of hydrates [13] occurs and it induces a temperature increase; there is a significant change in the temperature rate ($\partial T/\partial t = 31.9\,^{\circ}C/h$) and both temperature and the AE hit rate reach their maximum values ($T^{max} = 55\,^{\circ}C$, $t_T^{Max} = 5.61$ h, $\partial T/\partial t = 1320$ hits/h). As the understanding of the mechanisms inducing AE activity during this period is essential for the rest of the study, it has been shown [13] that numerous phenomena acting during the hydration process can be identified. We can quote in a non-exhaustive way:

(1) Capillary effect,
(2) Growth of crystalline phases,
(3) Fitting of hydrates due to tangling,
(4) Microcracking due to stress relaxation induced by shrinkage or drying.

These acoustically emissive mechanisms, and especially both the growth of crystalline phases and the tangling of hydrates, have a significant contribution to the mechanical behaviour of the set material. In terms of energy released the quoted mechanisms from (1) to (4) have been classified in increasing order.

The last period from 5.94 to 24 h corresponds to a lower value of the hit rate compared to the previous one since it is equal to 2.54 hits/h.

Fig. 7b shows differences in the evolution of the AE and temperature characteristics for cement B (55 days old). As already said, we observe a lower value of the total number of hits which denotes a lower acoustic activity during the setting process. As the number of hits can be considered as the acoustic activity of the phenomena, the number of counts can be associated to the global energy generated by the phenomena. In fact, for the same AE activity, the higher the energy it emits, the higher the amplitude and the longer its duration, and consequently the most numerous the counts, are. From data in Table 2, it turns out that the average total number of counts is lower for cement B than for cement A (1500 < 3300). These observations (hits and counts number) demonstrate that the hydration of cement B generates less acoustic activity and releases less energy than the hydration of cement A. Other

Table 2
AE and temperature features determined for cements A and B

Name	Duration of storage (days)	AE features				Temperature features			
		Average total number of hits	Average total number of counts	t_{AE}^{Start} (h)	$\frac{\partial H}{\partial t}$ (hit/h) (associated time period)	t_T^{Start} (h)	t_T^{Max} (h)	$\frac{\partial T}{\partial t}$ (°C/h) (associated time period)	T^{Max} (°C)
Cement A	2	680	3300	4.92	1320 (5.53 h–5.94 h) 2.6 (5.94 h–24 h)	2.70	5.61	5.3 (2.7 h–4.91 h) 31.9 (4.91 h–5.61 h)	55
Cement B	55	310	1500	4.76	129.4 (4.76 h–6.11 h) 25.6 (6.11 h–9.31 h) 117.4 (9.31 h–10.02 h) 4.2 (10.02 h–24 h)	4.71	7.18	11.2 (4.71 h–6.48 h) 14.7 (6.48 h–7.18 h)	46

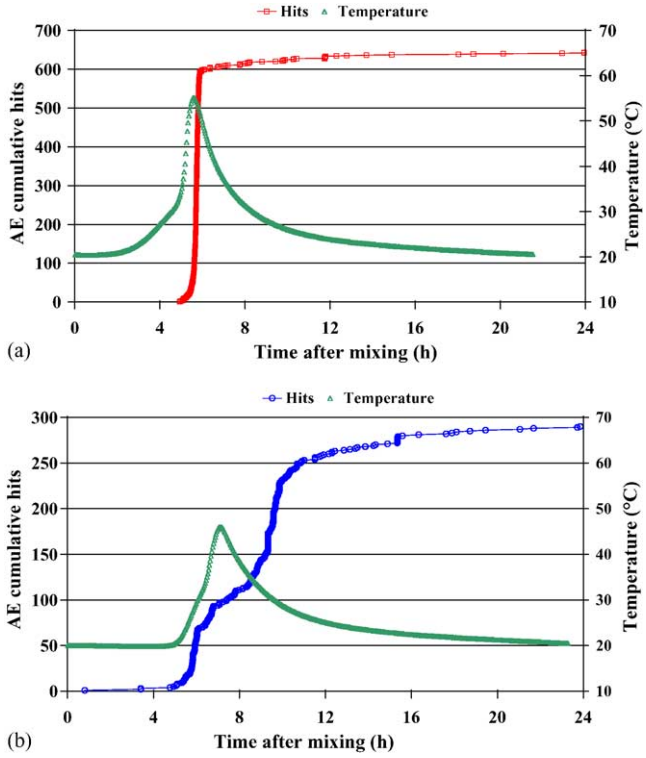

Fig. 7. (a) AE cumulative hits and internal temperature as a function of time after mixing for cement A. (b) AE cumulative hits and internal temperature as a function of time after mixing for cement B.

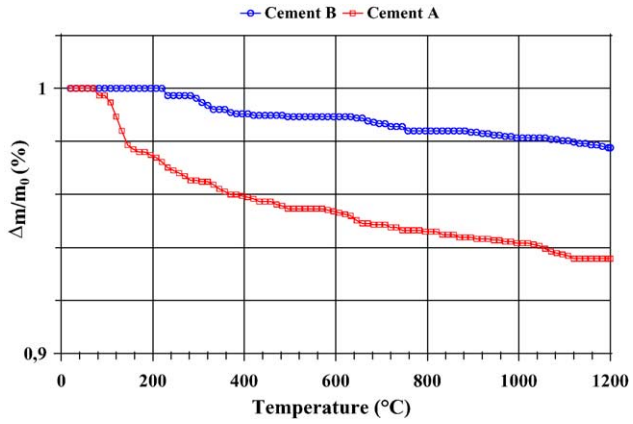

Fig. 8. Weight-loss curves for cement A and cement B upon heating (heating rate: 5 °C/min).

differences between the two cements occur. If we look at the variation of the AE hits for both cements, three distinctive stages can be identified. However, the second period, from approximately 4.76 to 10 h, presents an evolution in several stages. Indeed, during this time, three different values of the AE hit rate can be calculated (Table 2). The first and the third calculated rates seem to be of the same order (129 and 117 hits/h). The intermediate one (from 6.11 to 9.31 h) is reduced (25.6 hits/h) and it could probably indicate that a kind of "pause" is taking place in the hydration process. This AE evolution, in three steps, can also be interpreted through the analysis of the internal temperature variations. For cement B (Fig. 7b and Table 2), $t_T^{\text{Start}} \approx t_{\text{AE}}^{\text{Start}}$, $T^{\max} = 46\,^{\circ}\text{C}$ and $t_T^{\text{Max}} = 7.18$ h. The temperature reaches its maximum (lower than cement A: 55 °C) later than cement A. These results indicate that the reactivity of cement A and cement B differ. It is important to remember that only the duration of storage is different for the two cements. A thermogravimetric analysis (heating rate = 5 °C/min) was then performed in order to characterise the initial state of the anhydrous cement powder. The results are presented in Fig. 8. As we can see, cement A exhibits a notable weight-loss between 100 and 600 °C. The weight-loss is less important for cement B and starts at 200 °C. Two hypothesis can explain these differences:

- At a volumic scale, small hydrated germs are present in the anhydrous powder and participate in a better control of the setting behaviour of the paste. These germs decompose when the raw material is heated. During storage, these small hydrated germs can transform into thermally more stable phases that can modify the kinetics of the hydration process.
- At a surface scale, ageing conditions can deteriorate the intrinsic surface reactivity of the anhydrous grains. This can also leads to changes in the hydration process including delayed dissolution of anhydrous grains, slow precipitation or disturbed growth of hydrated phases.

At this stage of the study, some hypothesis, concerning the AE response of the cement at young age and its correlation with the mechanical behaviour when it is set, can be examined. Between all the mechanisms that can be active and potentially acoustically emissive, the ones that seem to be most active and most energetic are the fitting of hydrates, due to tangling, and the microcracking, due to stress relaxation induced by shrinkage or drying.[13] The consequence of these two mechanisms on the mechanical behaviour of the set material seems to be opposite. In the first case, it can favours an efficient rigidification of the solid skeleton in the paste and leads, even after the setting, to an increase of the mechanical strength. The second mechanism corresponds to the damage of the set material and the density of microcracking reduces both the rigidity and the strength of the set cement. Considering these interpretations, two hypotheses are proposed:

1. The level of AE is closely related to the efficiency of hydrates tangling and the associated mechanical properties are consequently high,
2. The level of AE is closely related to the microcracking density and the associated mechanical properties are consequently reduced.

3.2. Mechanical testing

In order to check these propositions, indirect tensile tests were conducted on several samples of the set cement (A and

Table 3
Mechanical features determined for cements A and B

Name	Duration of storage (days)	Mechanical characteristics	
		Average experimental rigidity (F/δ in N/mm) and scattering	Average tensile strength (σ_t in MPa) and scattering
Cement A	2	10215 (10.1%)	4.11 (6.5%)
Cement B	55	1329 (6.7%) (I) 5071 (7.5%) (II)	2.45 (2.7%)

For cement B, (I) and (II) correspond to the periods sighted in Fig. 9 and where two different values of the experimental rigidity has been calculated.

B). Fig. 9 and Table 3 present the obtained results. As we can see, the mechanical behaviour of cement A is different from that of cement B. The values of the experimental rigidity and the maximum strength are the highest for cement A (10215 N/mm > 5071 N/mm; 4.11 MPa > 2.45 MPa). Moreover, cement A exhibits a brittle like behaviour (linear variation of load with respect to the displacement and sudden fall of the strength related to the fracture of the specimen). For cement B, the load–displacement evolution probably indicates the occurrence of a high level of damage initially present in the set material. The final variations of the load for this cement can be interpreted as the propagation of the microcracking leading the catastrophic failure of the sample. Fig. 10a and b, which present the fracture aspects of the cement A and B samples, respectively, confirm the observation made on the load displacement curves. With respect to the hypotheses proposed above and the results of the mechanical testing, it appears that the first hypothesis is valid. Indeed, we observe a high level of AE activity associated with high mechanical properties. In the present case, the acoustic emission seems to be probably more likely related to a cohesive phenomenon (tangling of hydrates) than a damage process (microcracking). Even though, the two contributions (tangling of hydrates and microcracking) are active in both specimen, in cement A, the predominant mechanism seems to be the tangling of hydrates while in cement B, microcracking is playing an important role.

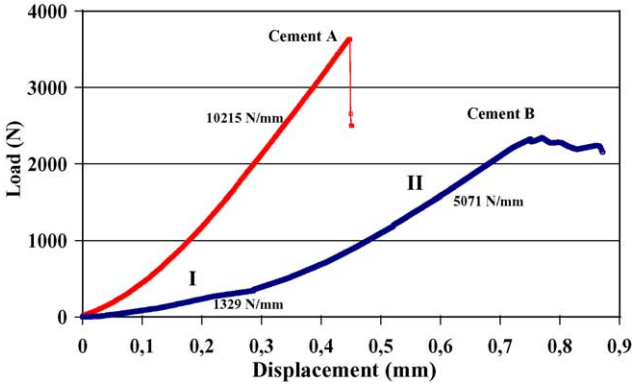

Fig. 9. Load–displacement curves from indirect tensile test for cement A and cement B.

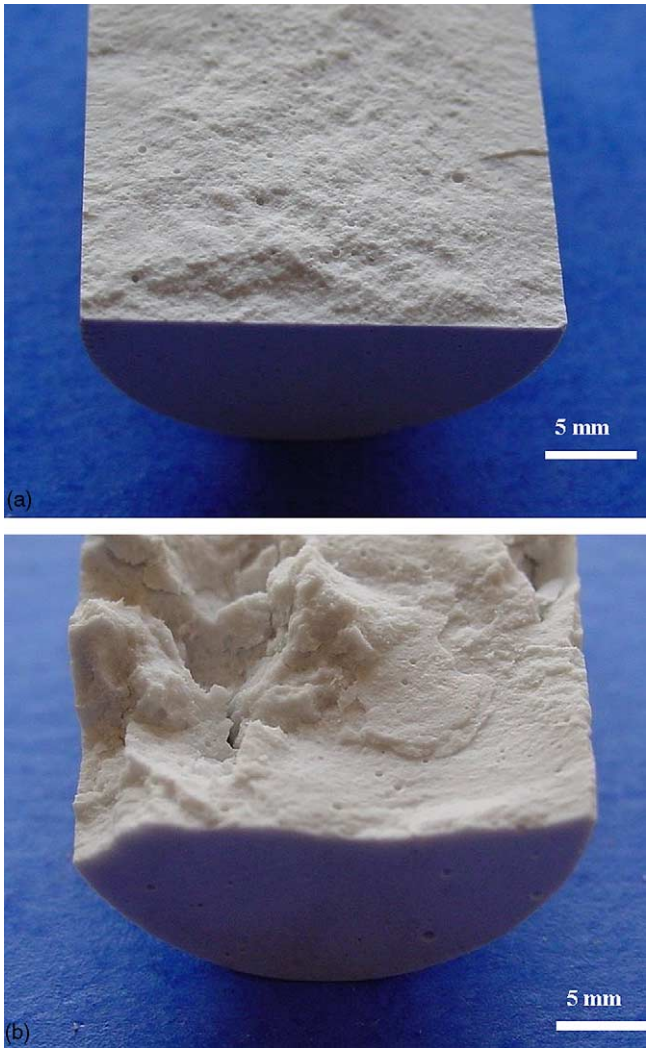

Fig. 10. Typical fracture aspect for sample after indirect tensile test (Brazilian test): (a) cement A and (b) cement B.

4. Conclusion

The results reported in this paper demonstrate that AE technique can be considered as a valuable tool not only to characterise the early hydration of a cement paste but also to predict the mechanical behaviour of the set cement. Quali-

tative observations and quantitative measurements enable to propose some conclusions:

- AE activity recorded during the setting allows to follow the build-in mechanism of the paste and to detect a potential disruption of the hydration process (in association with temperature measurement).
- Some the AE recorded signals seem to be related to the tangling of hydrates leading to the rigidification of the paste. Differences in surface reactivity of the starting materials influence upon the hydration process and, consequently, the AE response.
- Based on the experiments, the ageing conditions (duration of storage) of the anhydrous phase have a notable influence on the mechanical performances of the set material and can, with a good reliability, be detected and forecasted by AE monitoring.

This work opens interesting perspectives like real-time monitoring which can be applied to fairly large specimens (cement, mortars or concrete), in order to predict the mechanical characteristics of the set materials.

References

1. Scrivener, K. L., Cabiron, J. L. and Letourneux, R., High-performance concretes from calcium aluminate cements. *Cem. Concr. Res.*, 1999, **29**(29), 1215–1223.
2. Scrivener, K. L., Historical and present day applications of calcium aluminate cements. In *Proceedings of Calcium Aluminate Cements, 2001*, ed. R. J. Mangabhai and F. P. Glasser, 2001, pp. 3–23.
3. Gessner, W., Recent researches on calcium aluminate hydration. In *Proceedings of Calcium Aluminate Cements 2001*, ed. R. J. Mangabhai and F. P. Glasser, 2001, pp. 151–154.
4. Fujii, K., Kondo, W. and Ueno, H., Kinetics of hydration of monocalcium aluminate. *J. Am. Ceram. Soc.*, 1986, **69**(4), 361–364.
5. Edmonds, R. N. and Majumdar, A. J., The hydration of monocalcium aluminate at different temperatures. *Cem. Concr. Res.*, 1988, **18**(2), 311–320.
6. Cong, X. and Kirkpatrick, R. J., Hydration of calcium aluminate cements: a solid-state ^{27}Al NMR study. *J. Am. Ceram. Soc.*, 1993, **76**(2), 409–416.
7. Barnes, P., Clark, S. M., Hausermann, D., Henderson, E., Fentiman, C. H., Muhamad, M. N. *et al.*, Time-resolved studies of the early hydration of cements using synchrotron energy-dispersive diffraction. *Phase Transitions*, 1992, **39**, 117–128.
8. Rashid, S., Barnes, P., Bensted, J. and Turrilas, X., Conversion of calcium aluminate cement hydrates re-examined with synchrotron energy-dispersive diffraction. *J. Mater. Sci. Lett.*, 1994, **13**, 1232–1234.
9. Rashid, S. and Turrillas, X., Hydration kinetics of $CaAl_2O_4$ using synchrotron energy-dispersive diffraction. *Thermochim. Acta*, 1997, **302**, 25–34.
10. Mayfield, B. and Bettison, M., Ultrasonic pulse testing of high alumina cement concrete. *Concrete*, 1974, 36–38.
11. Boumiz, A., Vernet, C. and Cohen-Tenoudji, F., Mechanical properties of cement and mortars at early ages. *Adv. Cem. Bas. Mater.*, 1996, **1**, 94–106.
12. Chotard, T., Gimet-Bréart, N., Smith, A., Fargeot, D., Bonnet, J. P. and Gault, C., Application of ultrasonic testing to describe the hydration of calcium aluminate cement at the early age. *Cem. Concr. Res.*, 2001, **31**, 405–412.
13. Chotard, T., Smith, A., Rotureau, D., Fargeot, D. and Gault, C., Acoustic emission characterisation of calcium aluminate cement hydration at the early age. *J. Eur. Ceram. Soc.*, 2003, **23**, 387–398.
14. Maev, R. G., Shao, H. and Maeva, E. Y., Thickness measurement of a curved multilayered polymer system by using an ultrasonic pulse-echo method. *Mater. Chart*, 1998, **41**, 97–105.
15. Chang, L. S., Chuang, T. H. and Wei, W. J., Characterization of alumina ceramics by ultrasonic testing. *Mater. Chart*, 2000, **45**, 221–226.
16. Gür, C. H. and Ogel, B., Non-destructive microstructural characterization of aluminium matrix composites by ultrasonic techniques. *Mater. Chart*, 2001, **47**, 227–233.
17. Hamstad, M. A., A review: acoustic emission, a tool for composite materials studies. *Exp. Mech.*, 1986, **26**, 7–13.
18. Roget, J., Acoustic emission: valuable applications and future trends. In *Proceedings of the Fouth European Conference on Non-destructive Testing, Vol 4*, ed. J. M. Farley and R. W. Nichols. London, 1987.
19. Hamstad, M. A., Thompson, P. M. and Young, R. D., Flaw growth in alumina studied by acoustic emission. *J. Acoust. Emis.*, 1987, **6**, 93–97.
20. Bakuckas, J. G., Prosser, W. H. and Johnson, W. S., Monitoring damage growth in titanium matrix composites using acoustic emission. *J. Comp. Mater.*, 1994, **28**, 305–328.
21. Berkovits, A. and Fang, D., Study of fatigue crack characteristics by acoustic emission. *Eng. Fract. Mech.*, 1995, **51**, 401–416.
22. Havlicek, F. and Crha, J., Acoustic emission monitoring during solidification processes. *J Acoust. Emis.*, 1999, **17**, 3–4.
23. Coddet, C., Chretien, J. F. and Beranger, G., Investigation on the fracture mechanism of oxide layers growing on titanium by acoustic emission. *Titanium and Titanium Alloys: Scientific and Technological Aspects, Vol 2*. 1982, pp. 1097–1105.
24. Prosser, W. H., Jackson, K. E., Kellas, S., Smith, B. T., McKeon, J. and Friedman, A., Advanced waveform-based acoustic emission detection of matrix cracking in composites. *Mater. Eval.*, 1995, 1052–1058.
25. Suzuki, H., Takemoto, M. and Ono, K., The fracture dynamics in a dissipative glass fibber/epoxy model composite with AE source simulation analysis. *J. Acoust. Emis.*, 1996, **14**, 35–50.
26. Barré, S. and Benzeggagh, M. L., On the use of acoustic emission to investigate damage mechanisms in glass-fibre-reinforced polypropylene. *Compos. Sci. Tech.*, 1994, **52**, 369–376.
27. Ohtsu, M., Tomoda, Y. and Fujioka, T., Estimation of initial damage in concrete by acoustic emission. In *Proceedings of the Fourth Far East Conference on NDT, Vol 1*. Singapore, 1997, pp. 151–156.
28. Chen, H. L., Cheng, C. T. and Chen, S. E., Determination of fracture parameters of mortar and concrete beams by using acoustic emission. *Mater. Eval.*, 1992, 888–894.
29. Maji, A. and Shah, S. P., Process zone and acoustic emission measurement in concrete. *Exp. Mech.*, 1988, 27–33.
30. Li, Z. and Shah, S. P., Localisation of microcracking in concrete under uniaxial tension. *ACI Mater. J.*, 1994, 372–381.
31. Yuyama, S., Okamoto, T., Shigeishi, M. and Ohtsu, M., Quantitative evaluation and visualisation of cracking process in reinforced concrete by a moment tensor analysis of acoustic emission. *Mater. Eval.*, 1995, 751–756.
32. Ohtsu, M., Okamoto, T. and Yuyama, S., Moment tensor analysis of acoustic emission for cracking process concrete. *ACI Struct. J.*, 1998, 87–95.
33. Uomoto, T., Application of acoustic emission to the field of concrete engineering. *J. Acoust. Emis.*, 1987, **6**, 137–144.
34. Darwell, B. W., Review: uniaxial compression tests and the validity of indirect tensile strength. *J. Mater. Sci.*, 1990, **25**, 757–780.